Effect of hydrogen pickup on fracture behaviour of stainless steels

R.C. Prasad[1], S. Roychowdhury[2], V. Kain[2]
[1]Indian Institute of Technology, Powai, Mumbai, India; [2] Bhabha Atomic Research Centre, Mumbai, India

Abstract: Hydrogen pickup influences plasticity and fracture properties and is one of the major causes for materials failure. In this study effect of hydrogen precharging on the initiation fracture toughness and crack growth resistance have been studied for austenitic stainless steel grade SS 304 and duplex stainless steel grade 2205. Fatigue precracked specimens were cathodically precharged and fracture toughness testing was done as per ASTM standard. Initiation J-integral could not be obtained by standard methods. Stretch zone width (SZW) was measured to get crack initiation toughness. After hydrogen charging SZW formation was not observed. Crack tip opening displacement (CTOD) showed a reduction due to hydrogen charging in both the grades of stainless steels. Crack growth resistance also reduced due to hydrogen pickup. It is concluded that in stainless steels hydrogen pickup leads to a reduction in the initiation fracture toughness and the crack growth resistance. CTOD is observed to be a better toughness criterion for study of hydrogen pickup effect.

1.0 Introduction

Hydrogen - deformation interaction at crack tip influences plasticity and is one of the major causes of failures in steels. The effect of hydrogen on mechanical properties have been widely investigated [1-3] using conventional mechanical tests. Considerable loss of mechanical properties, plasticity and ability to withstand static sustained and dynamic cyclic loading due to hydrogen absorption is reported particularly for high strength steels. After severe local deformation at the crack tip, fracture initiates that is followed by a period of stable crack growth [4]. This information about the crack growth kinetics in air or in the working environment is an important parameter in the residual life assessment of engineering components. The crack growth resistance and fracture toughness data like J_{IC}, K_{IC}, CTOD are important input parameters for constructing failure assessment diagrams of engineering components, which gives the damage tolerance of components against fracture. The tearing modulus also gives the crack growth resistance which helps in finding the point of crack growth instability. CTOD values have been reported to be very accurate in measuring the effects of hydrogen rather than the SSRT of uniaxial tensile specimens [5].

The effect of hydrogen precharging on the fracture behaviour of a single phase austenitic stainless steel grade AISI SS 304 and a duplex stainless steel (DSS) Grade 2205 has been described in this paper. This study illustrates that austenitic stainless steels, which are considered to be relatively insensitive to hydrogen attack (HA), show a drastic reduction in the initiation fracture toughness as well

as the propagation toughness. The estimation of the influence of HA on the stretch zone width in these steels has also been attempted in this study.

2.0 Experimental

The composition of the DSS and the austenitic stainless steel used in this study in given in table 1. Image analysis had shown [6, 7] the presence of the phases, austenite and ferrite in the DSS in almost equal volume fraction (austenite: ferrite: 49.2: 50.8). For SS 304 equiaxed grain structure was observed. The microstructure for the SS 304 indicated a low susceotibility to sensitization. The degree of sensitization obtained by electrochemical potentiokinetic reactivation technique [6, 7] was 0.06% and the steel has "dual" structure. Such extent of sensitization is expected in the as received condition. Figure 1 shows the microstructure of both the DSS and the SS 304.

Table1: Chemical composition of the stainless steels used

	C	Cr	Ni	Mo	Mn	Si	P	S	N	Fe
DSS	0.023	22.17	4.73	2.73	1.19	0.77	0.027	0.002	0.12	bal.
SS 304	0.05	21	8.45	---	---	1.31	0.005	0.005	---	bal.

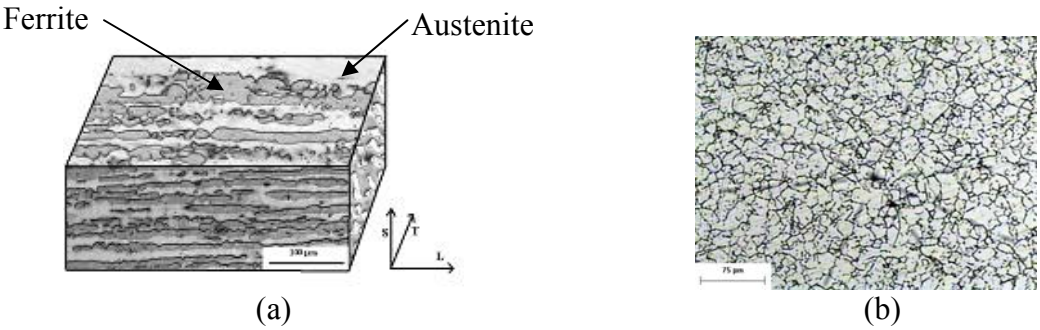

(a) (b)

Figure 1. Microstructure of (a) duplex stainless steel, (b) SS 304

The initial material was in the form of 12 mm thick plate from which CT specimens were machined as per the specifications [8] laid down by ASTM E-1820 (B-8 mm, W-33.5 mm). Specimens of TL orientation were used for the DSS so that the crack plane is perpendicular to the rolling plane but parallel to the rolling direction. The material was used in the as received condition.

The CT specimens were polished on both the sides to a finish of 6 micron. The CT specimens were then cathodically charged with hydrogen at room temperature in the galvanostatic mode at a constant current density of 30 mA/cm^2. Charging was done in 1N H_2SO_4 + 30mg/l As_2O_3. The hydrogen charging was done for a total of 192 hrs (8 days) out of which 28 hrs of charging was done by applying a tensile load of 100 kg (1 kN) so as to assist hydrogen diffusion under stress gradient at the crack tip. The solution was changed after every 28 hours. After

hydrogen charging the fracture toughness testing was done with a minimum time delay to prevent loss of hydrogen due to diffusion.

The ASTM standard E-1820 was followed for the fracture toughness tests. The CTOD-R and J-R curves were obtained from the load-COD plots and the crack growth resistance dδ/da and dJ/da were obtained by fitting a straight line between crack extension of 0.5 mm and 1.5 mm. The CT specimens were fatigue post cracked after fracture toughness testing and the fracture surface was observed in the scanning electron microscope.

3.0 Results and Discussion

The fracture toughness testing was done by the single specimen multiple unloading techniques. From the load – COD data, the J-R and the CTOD-R curves were obtained. The crack initiation toughness and the crack growth resistance was estimated from these curves. Figure 2 (a, b) shows the combined J-R plot obtained from the test data for the as received specimens without hydrogen charging and for the specimens after hydrogen charging for both the DSS and the austenitic stainless steel. It was observed that all the data points in the J-R curve for both the stainless steels fall beyond the region of validity as specified in the ASTM standard in both the as received and the hydrogen charged condition. Similar observations have been reported earlier for high toughness steels [9-12].

Table-2 lists the crack growth resistance values for both the stainless steels with and without hydrogen charging. It is clear that hydrogen pickup has resulted in the reduction in the crack growth resistance as is evident from the reduction in dJ/da values and also the fall in the J-R curves. The distribution of the hydrogen content is expected to be non uniform in the regions ahead of the crack tip as the hydrogen charging was done under the application of load. The hydrogen content is expected to be maximum at the crack tip region decreasing with increasing distance from the crack tip. The absence of the SZW formation after hydrogen charging indicates that the embrittlement due to hydrogen pickup is high at the crack tip region and once the crack crosses this region of high hydrogen concentration, the embrittlement is governed by the bulk hydrogen concentration which reduces the crack growth resistance. Figure 3 (a - d) shows the crack tip before and after hydrogen charging. The figure clearly illustrates that the SZW formation has been impeded due to hydrogen charging in both the stainless steels. The initiation fracture toughness can be obtained by the value of the SZW for the steel without any hydrogen charging. But the initiation fracture toughness could not be obtained after hydrogen charging for comparing the effect of hydrogen pickup on the initiation fracture toughness. The J-integral approach is thus, an effective tool to study the effect of hydrogen pickup on the crack propagation toughness but the effect of hydrogen pickup on the crack initiation toughness cannot be studied using this approach.

The same load-COD data was used to obtain the CTOD-R plot as per the ASTM standard. Figure 4 (a – d) shows the CTOD-R plots along with the exclusion lines

for both the duplex stainless steel and the austenitic stainless steel with and without hydrogen. The figures clearly indicate that the CTOD values are within the valid region for both the as received and after hydrogen charging. The initiation CTOD values could be obtained from the CTOD-R plots. The dδ/da value that indicates the crack growth resistance was also obtained from the CTOD-R plots. Table-3 lists the initiation CTOD and the dδ/da values. There is a reduction in the initiation CTOD values by 15% for SS 304 and 11% for DSS-TL specimens. While the dδ/da showed a reduction of 34% for SS 304 and 9% for DS-TL specimens.

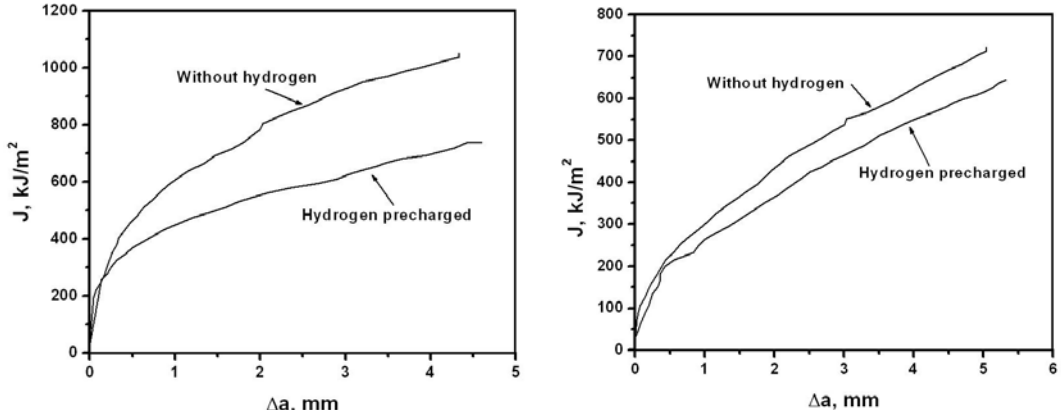

(a) (b)

Figure 2. J-R plot in the as received condition (without hydrogen) and after hydrogen charging for (a) duplex stainless steel, [7] b) SS 304

Table – 2: dJ/da values for the hydrogen precharged steels

	After Hydrogen Charging (MPa)	Without Hydrogen Charging (MPa)
SS 304	108	140
DSS - TL	87	102

Duplex stainless steel is a dual phase stainless steel containing 50:50 volume fraction of austenite and ferrite while the austenitic stainless steel, SS 304 is a single phase stainless steel. The phase morphology and distribution also affects the fracture toughness and the effect of hydrogen pickup also depends on this. Figure 5 (a, b) shows the J-R curves and CTOD-R curves for both the stainless steel with and without hydrogen. Both the figures indicate the reduction in the crack growth resistance due to hydrogen pickup. Figure 5 (a) shows that the J-R

curve for duplex stainless steel is above the J-R curve for SS 304. Even after hydrogen charging similar effect is observed. This is an indication that the resistance to crack growth is more in the dual phase duplex stainless steel as compared to single phase austenitic stainless steel. Similar trend is seen in the CTOD – R curve, where the resistance to crack growth is more in the dual phase steel as compared to the single phase steel. This may be attributed to the morphology of the two phases present in the duplex stainless steel. Figure 6 (a, b) shows the fracture surface of the duplex stainless steel as well as a schematic of the morphology of the phases present and the fracture surface of the austenitic stainless steel. No difference in the fracture surface was observed for the as received and the hydrogen precharged specimens in the duplex stainless steel as well as SS 304. It has been reported [3, 13] that hydrogen does not change the appearance of the fracture surface but it causes a change in the appearance of the dimples. The dimple size and density may change due to the presence of hydrogen. But in this investigation no such change was apparent apart from the fact that the as received samples showed SZW formation while the hydrogen precharged ones didn't show any SZW formation.

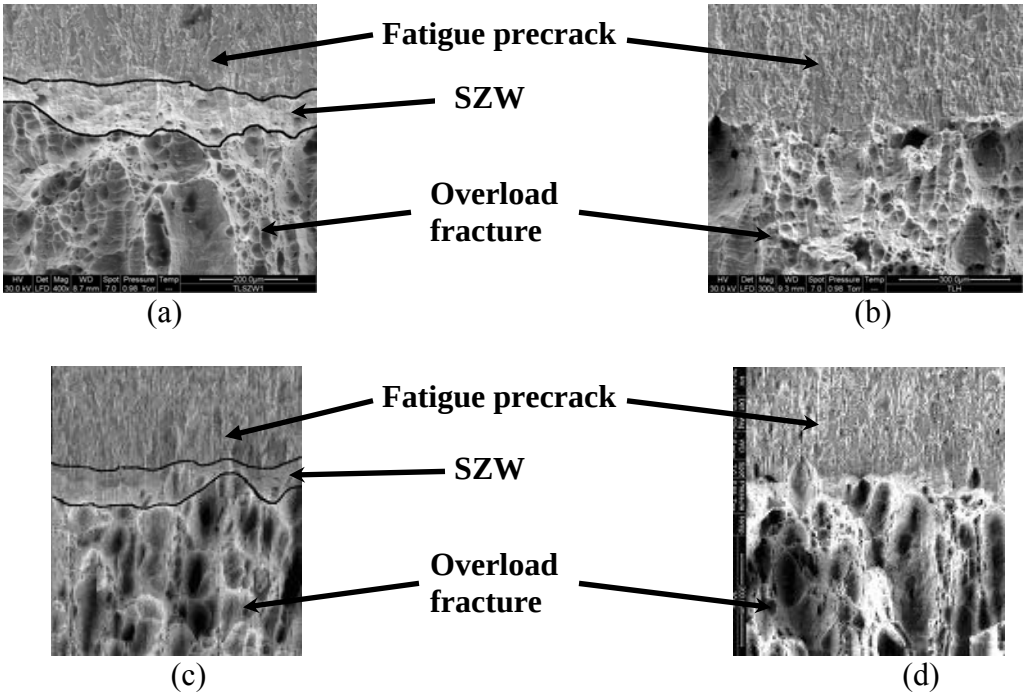

Figure 3. Fracture surface showing the crack tip region after fracture toughness testing (a) duplex stainless steel without hydrogen showing formation of SZW, [7] (b) duplex stainless steel after hydrogen showing no SZW formation, [7] (c) SS 304 without hydrogen showing SZW formation, (d) SS 304 after hydrogen charging showing no SZW formation.

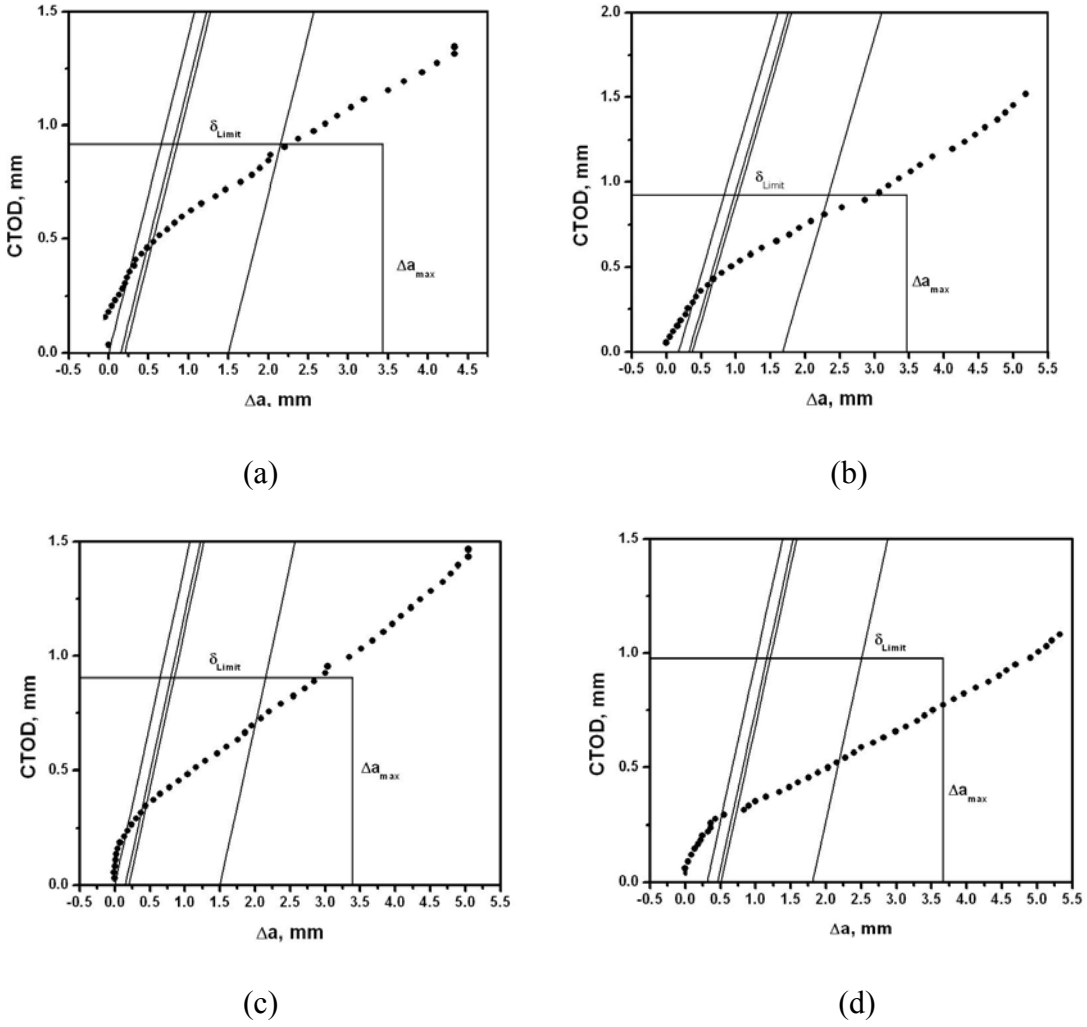

Figure 4. CTOD-R plots along with the exclusion lines for duplex stainless steel (a) without hydrogen, [7] (b) after hydrogen charging, and for austenitic stainless steel type 304 [7] (c) without hydrogen (d) after hydrogen charging. All the data points for both the stainless steels with and without hydrogen lie in the valid region as specified by the standard.

Table – 3: Initiation CTOD and dδ/da values

	Initiation CTOD (mm)		dδ/da	
	As received	Hydrogen precharged	As received	Hydrogen precharged
SS 304	0.333	0.284	0.2237	0.1469
DSS – TL	0.482	0.430	0.2590	0.2380

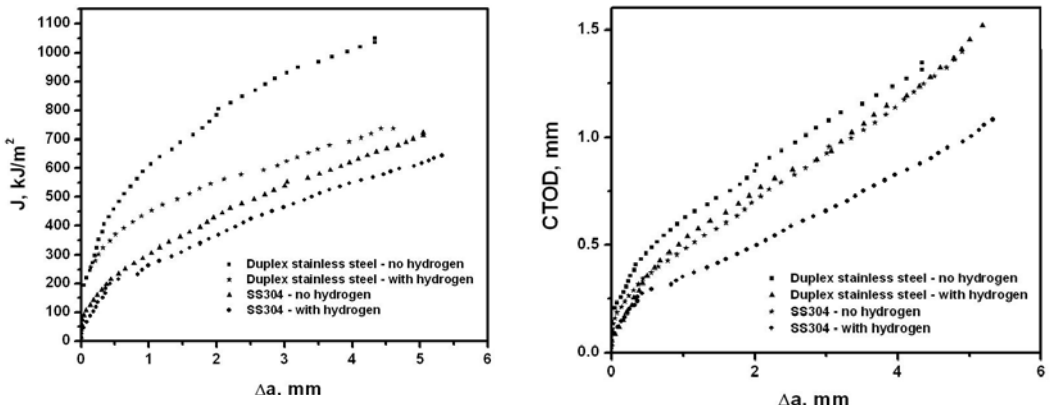

(a) (b)

Figure 5. Plots showing (a) J-R curves and (b) CTOD-R curves, for both the stainless steels with and without hydrogen.

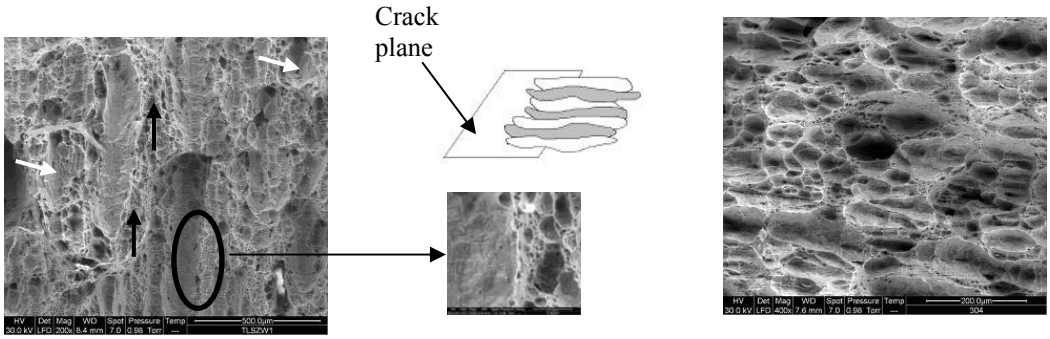

(a) (b)

Figure 6. Fracture surface after hydrogen charging and fracture toughness testing of (a) duplex stainless steel showing quasi-cleavage (white arrow) and microvoid coalescence (black arrow) and orientation of the crack plane with respect to the morphology of the phases (austenite and ferrite). The boundary between the two regions can be seen in the inset indicating crack growth along the austenite – ferrite phase boundary on the left side and microvoid coalescence on the right side. (b) SS 304 showing ductile failure by microvoid coalescence.

Distinct difference in the fracture surfaces is evident from the fractographs. The fractograph for the duplex stainless steel specimen (figure 6a) show both regions of cleavage or quasi-cleavage (white arrow) and microvoid coalescence (black arrow). The crack extension occurs by cleavage or quasi-cleavage of the ferrite regions while the austenite domains fail by microvoid coalescence. There is indication of the crack extension along the α-γ phase boundaries as seen in the left side region in the inset. In the SS 304 the fracture surface (figure 6b) indicates the occurrence of predominant microvoid coalescence. There is no evidence of any cleavage fracture even after hydrogen charging.

For a composite material consisting of a brittle and a ductile component, the most important influencing factor for the crack growth resistance is the arrangement of the brittle and the ductile domains and not the volumetric fraction of the

components. In the TL orientation in the duplex stainless steel the crack plane is in the longitudinal direction (Figure 6 (a). Hence, long regions of ferrite phase fields as well as ferrite/austenite phase boundaries are available. When the crack is growing it encounters both the ductile austenite phase as well as the brittle ferrite. Crack will grow with greater ease though the ferrite phase but once it encounters an austenite phase field it will get deflected and the crack will start growing along the austenite ferrite phase boundary. This frequent deflection of the crack front leads to increased fracture toughness. But the crack growth resistance will be lower (as indicated by a lower dJ/da value) due to the ease in the crack growth. For a given crack extension, the J value for type 304 stainless steel is lower than that of DSS but the crack growth resistance for SS 304 is higher than DSS TL specimens for the range of crack extension of 0.5 mm to 1.5 mm.

In the single phase SS 304 the crack deflection does not occur hence the fracture toughness will be lower but the crack growth resistance will be higher as there is no easy path for the crack to grow. Figure 5 (a) shows that the J-R curve for duplex stainless steel with and without hydrogen is above the J-R curve for SS 304 indicating greater toughness but the crack growth resistance in duplex stainless steel is lower than that in the austenitic stainless steel (Table 2). This may also be due to the enhanced plasticity ahead of the crack tip in the ductile single phase SS 304 specimens while the DSS TL specimens will have restricted crack tip plasticity due to the presence of long regions of weak austenite/ferrite phase boundaries and also brittle ferrite phase in the crack plane. The crack can easily follow the weak path leading to reduced crack growth resistance. Similar trend was also observed in the CTOD-R plots where the curves for the duplex stainless steel was above that for SS 304 indicating enhanced toughness in the duplex stainless steel. However, the $d\delta/da$ did not show any trend similar to what was observed in dJ/da.

The effect of hydrogen on the dislocation mobility and thus the proof stress has been widely reported [14-16]. Both increase and a decrease in the proof stress for tensile specimens have been reported due to the effect of hydrogen charging, irrespective of the crystal structure leading to a gross reduction in the ductility. Increase in the proof stress is due to a greater extent of slip localization than enhancement of dislocation mobility due to hydrogen pickup [14-15]. And the reverse is true for reduction in the proof stress. In duplex stainless steels it has been reported that hydrogen pickup results in an increase in the hardness values which in due to the increase in the yield strength [7]. This leads to a reduction in the fracture toughness. A similar trend is also expected in the austenitic stainless steel. However, in austenite phase of the duplex stainless steel and the single phase austenite stainless steel martensitic transformation due to hydrogen charging is also expected leading to embrittlement. In the present investigation it seems hardening is due to a greater extent of slip localization than enhancement of dislocation mobility and also due to martensite transformation leading to an overall reduction in the fracture toughness due to hydrogen pickup.

4.0 Conclusions

The following conclusions can be drawn from the present investigation.

1. Both DSS and ASS are susceptible to HE as is evident from the reduction in the crack growth resistance (dJ/da and dδ/da) and reduction in initiation CTOD.

2. Fracture toughness of DSS depends on the orientation of the crack plane with respect to the elongated ferrite and austenite phase domains more than the volume fraction of the ductile and brittle phases.

3. Fractographs reveal cleavage/quasi cleavage fracture in ferrite and microvoid coalescence in the austenite. In duplex stainless steel crack growth also occurs significantly along the austenite/ferrite phase boundaries. In SS 304 the microvoid coalescence was the predominant mode of fracture.

4. Fracture toughness is higher in the duplex stainless steel as compared to the single phase austenitic stainless steel but the crack growth resistance is higher in the single phase austenitic stainless steel.

5.0 References

1. J. Woodtli, R. Kieselbach, Damage due to hydrogen embrittlement and stress corrosion cracking, Engineering failure analysis, 7 (2000) 427-450.

2. S.M. Beloglazov, Pecularity of hydrogen distribution in steel by cathodic charging, Journal of alloys and compounds, 356-357 (2003) 240-243.

3. G.P. Tiwari, A. Bose, J.K. Chakraborty, S.L. Wadekar, M.K. Totlani, R.N. Arya, R.K. Fotedar, A study of internal hydrogen embrittlement of steels, Materials Science and Engineering A, 286 (2000) 269-281.

4. G.E. Dieter, Mechanical metallurgy, Mc Graw Hill Book Company, 1988.

5. S.C. Mittal, R.C. Prasad, M.B. Deshmukh, Effect of hydrogen on fracture of austenitic Fe-Mn-Al steels, The Iron and steel institute of Japan, 34 (1994) 211-216.

6. S. Roychowdhury, Environmental effects on the fracture toughness of stainless steels, M.Tech. thesis, Indian Institute of Technology, Bombay 2005.

7. S. Roychowdhury, V. Kain, R.C. Prasad, Environmental effects on the fracture toughness of a duplex stainless steel (UNS S31803), Corrosion, 63 (2007) 442-449.

8. ASTM international, Standard Test Method for Measurement of Fracture Toughness E-1820-99a, *Annual Book of standards,* Vol. 3.01. West Conshohocken, Pennsylvania.

9. E. Roos, U. Eisele, Determination of material characteristic values in elastic-plastic fracture mechanics by means of J-integral crack resistance curves, Journal of testing and evaluation, 16 (1988) 1.

10. K.F. Amouzouvi, M.N. Bassim, Determination of fracture toughness from stretch zone width measurement in predeformed AISI type 4340 steel, Materials science and engineering, 55 (1982) 257.

11. M.N. Bassim, Use of the stretch zone for the characterization of ductile fracture, Journal of materials processing technology, 54 (1995) 109.

12. O. Kolednik, M. Albrecht, M. Berchthaler, H. Germ, R. Pippan, F. Riemelmoser, J. Stampfl, J. Wei, The fracture resistance of a ferritic – austenitic duplex steel, Acta metallurgica et materialia, 44 (1996) 3307.

13. E. Herms, J.M. Olive, M. Puiggali, Hydrogen embrittlement of 316L type stainless steel, Materials Science and Engineering A, 272 (1999) 279-283.

14. I.M. Robertson, The effect of hydrogen on dislocation dynamics, Engineering fracture mechanics, 68 (2001) 671-692.

15. H.K. Birnbaum, Hydrogen effects on deformation – relation between dislocation behaviour and the macroscopic stress – strain behaviour, Scripta Metallurgica et Materialia, 31 (1994) 149-153.

16. P. Rozenak, I.M. Robertson, H.K. Birnbaum, HVEM studies of the effects of hydrogen on the deformation and fracture of AISI type 316 austenitic stainless steel, Acta metallurgica et materialia, 18 (1990) 2031-2040.